# Huntingtin Interacting Protein 1 Is a Clathrin Coat Binding Protein Required for Differentiation of late Spermatogenic Progenitors

DINESH S. RAO,[1] JENNY C. CHANG,[1] PRITI D. KUMAR,[1] IKUKO MIZUKAMI,[1] GLENNDA M. SMITHSON,[1]†
SARAH V. BRADLEY,[1] A. F. PARLOW,[2] AND THEODORA S. ROSS[1]*

*Division of Hematology and Oncology, Department of Internal Medicine, University of Michigan Medical School,
Ann Arbor, Michigan 48109-0936,[1] and National Hormone and Peptide Program, Harbor-UCLA Medical Center,
Torrance, California 90509[2]*

Huntingtin-interacting protein 1 (HIP1) interacts with huntingtin, the protein whose gene is mutated in Huntington's disease. In addition, a fusion between HIP1 and platelet-derived growth factor β receptor causes chronic myelomonocytic leukemia. The HIP1 proteins, including HIP1 and HIP1-related (HIP1r), have an N-terminal polyphosphoinositide-interacting epsin N-terminal homology, domain, which is found in proteins involved in clathrin-mediated endocytosis. HIP1 and HIP1r also share a central leucine zipper and an actin binding TALIN homology domain. Here we show that HIP1, like HIP1r, colocalizes with clathrin coat components. We also show that HIP1 physically associates with clathrin and AP-2, the major components of the clathrin coat. To further understand the putative biological role(s) of *HIP1*, we have generated a targeted deletion of murine *HIP1*. *HIP1*$^{-/-}$ mice developed into adulthood, did not develop overt neurologic symptoms in the first year of life, and had normal peripheral blood counts. However, HIP1-deficient mice exhibited testicular degeneration with increased apoptosis of postmeiotic spermatids. Postmeiotic spermatids are the only cells of the seminiferous tubules that express HIP1. These findings indicate that HIP1 is required for differentiation, proliferation, and/or survival of spermatogenic progenitors. The association of HIP1 with clathrin coats and the requirement of HIP1 for progenitor survival suggest a role for HIP1 in the regulation of endocytosis.

Originally identified by yeast two-hybrid screening for proteins that interact with Huntingtin, HIP1 is a 116-kDa cytosolic protein which is ubiquitously expressed and highly enriched in human and mouse brain tissue (14, 28). The true function of HIP1 remains unknown, but it has been shown to contain evolutionarily conserved sequences, including a leucine zipper motif and a carboxyl terminus with homology to TALIN, a cytoskeletal actin binding protein implicated in cell-substratum as well as cell-cell interactions (14). HIP1-related (HIP1r), the only known human homologue of HIP1, binds to actin through its TALIN homology region, colocalizes with clathrin pits, and, as shown recently, contains an epsin N-terminal homology (ENTH) domain (7, 8, 13). This latter domain binds to phosphatidylinositol-4,5-bisphosphate (PI4,5-P$_2$) as well as phosphatidylinositol-3,4,5-trisphosphate (PI-3,4,5-P$_3$) and may be important in regulating clathrin-mediated endocytosis. The yeast orthologue of *HIP1* and *HIP1r, SLA2P*, is essential for cellular growth as well the assembly of the cortical cytoskeleton (12). The similarities in protein sequence and predicted domains between HIP1, HIP1r, and Sla2p suggest an analogous role for HIP1 in the regulation of cytoskeletal and endocytic processes.

In addition to its possible involvement in endocytosis, HIP1 may play a role in the pathogenesis of Huntington's disease. It binds to the amino terminus of huntingtin in a region downstream of the polyglutamine sequence that undergoes expansion in Huntington's disease (28). The huntingtin-HIP1 interaction is weakened in huntingtin mutants with an expanded polyglutamine repeat, suggesting that in Huntington's disease, HIP1 is no longer able to bind to huntingtin (14). Therefore, the neruodegeneration observed in Huntington's disease maybe due in part to dysregulated HIP1 function (9). Huntingtin itself is a 350-kDa protein which is essential for normal embryonic development, including gastrulation, neurogenesis, and extraembryonic tissue formation (1, 3, 19, 29, 30). In addition, it has been suggested that huntingtin is necessary for normal hematopoiesis (18) and may function as an iron binding protein (10). Some of these abnormalities seen with the lack of functional huntingtin may also be attributable to the anomalous or unregulated activity of huntingtin-interacting proteins such as HIP1.

Further evidence for a role for HIP1 in cellular survival or proliferation was found when a t(5;7)(q33;q11.2) chromosomal translocation was cloned from a patient with chronic myelomonocytic leukemia (23). The N-terminal portion of the fusion protein encoded HIP1, and further studies with the HIP1/platelet-derived growth factor β receptor (PDGFβR) fusion protein showed that both the HIP1 and PDGFβR portions of the fusion were necessary for transformation. Even when the PDGFβR portion was constitutively activated by dimerization via the TALIN homology domain, it was not sufficient to transform cells (24, 25).

---

* Corresponding author. Mailing address: Division of Hematology and Oncology, Department of Internal Medicine, University of Michigan Medical School, Ann Arbor, MI 48109-0936. Phone: (734) 615-5509. Fax: (734) 647-9654. E-mail: tsross@umich.edu.
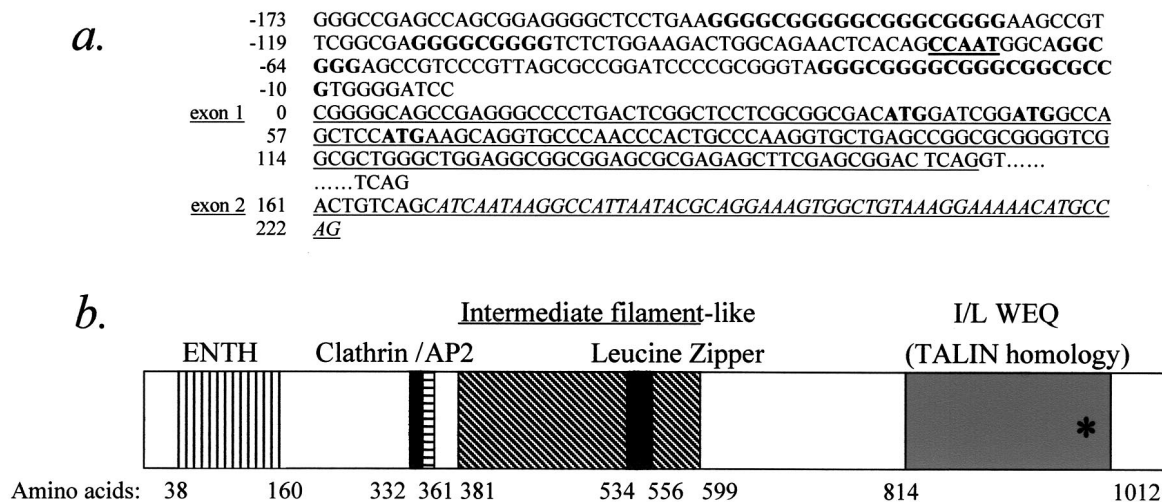† Present address: Curagen Corp., Bradford, CT 06405.

*a.*

```
        -173  GGGCCGAGCCAGCGGAGGGGCTCCTGAAGGGGCGGGGGCGGGCGGGGAAGCCGT
        -119  TCGGCGAGGGGCGGGGTCTCTGGAAGACTGGCAGAACTCACAGCCAATGGCAGGC
         -64  GGGAGCCGTCCCGTTAGCGCCGGATCCCCGCGGGTAGGGCGGGGCGGGCGGCGCC
         -10  GTGGGGATCC
exon 1    0  CGGGGCAGCCGAGGGCCCCTGACTCGGCTCCTCGCGGCGACATGGATCGGATGGCCA
         57  GCTCCATGAAGCAGGTGCCCAACCCACTGCCCAAGGTGCTGAGCCGGCGCGGGGTCG
        114  GCGCTGGGCTGGAGGCGGCGGGAGCGCGAGAGCTTCGAGCGGGAC TCAGGT......
             ......TCAG
exon 2  161  ACTGTCAGCATCAATAAGGCCATTAATACGCAGGAAAGTGGCTGTAAAGGAAAAACATGCC
        222  AG
```

*b.*



FIG. 1. Nucleotide sequence of the *HIP1* promoter, the newly identified exon 1, and domain structure of the HIP1 protein. (a) Promoter and coding sequence of *HIP1* exon 1. Promoter sequences are shown, with the CCAAT box underlined and bold and GC boxes in bold. Putative initiator methionines are shown in bold. The first of these contains the strongest Kozak consensus sequence (15). Only the italicized sequence was previously available through the National Center for Biotechnology Information. (b) HIP1 protein domains. The amino acid sequence of HIP1 exhibits homology to previously characterized domains in other proteins, as noted in the figure. Abbreviations: ENTH, epsin N-terminal homology; Clathrin, putative clathrin binding site; AP-2, putative AP-2 binding site; LZ, leucine zipper. The asterisk shows the breakpoint in the HIP1-PDGFβR fusion protein (23).

To better understand the biological role of *HIP1* and its role in disease, we have generated antibodies to HIP1 to assess its role in clathrin-mediated endocytosis. Using these antibodies, we report here that HIP1 colocalizes and physically associates with clathrin and AP2, the main components of the clathrin coat (11). Clathrin-mediated endocytosis requires several clathrin and AP-2 binding accessory proteins (26) to assemble a lattice at the plasma membrane for initiating and completing endocytosis. We propose here that HIP1 participates as one of these endocytic cofactors.

To begin to investigate the function HIP1 further, we have also created mice that have a targeted deletion in exons 2 to 7 of the *mHIP1* gene. In generating the necessary targeting vector, a putative promoter region and previously unknown 5' exon have been identified. Sequence analysis of the amino-terminal exons of *HIP1* demonstrates an ENTH domain, similar to that found in HIP1r (8, 13). Male *HIP1*-deficient mice exhibited degeneration of the seminiferous tubules of the testis, with excessive apoptosis of postmeiotic spermatids. The postmeiotic spermatids are the only cells of the seminiferous tubules that express HIP1. This suggests that HIP1 is required by spermatogenic progenitors at specific stages of development, perhaps to regulate clathrin trafficking or cytoskeletal rearrangements.

## MATERIALS AND METHODS

**DNA constructs.** The glutathione *S*-transferase (GST)-3'hHIP1 fusion construct that was used to generate anti-hHIP1 monoclonal antibodies contained GST fused in frame to HIP1 amino acid sequences starting at the internal *Eco*RI site (nucleotide 1250) and ending at the native stop codon (nucleotide 3010). The murine HIP1 antigen was a GST-mHIP1 fusion starting at mHIP1 nucleotide 1 and ending at nucleotide 1599.

**Antibody production.** The pGEX-3'HIP1 construct was used to express and purify human recombinant protein as described by the supplier of the pGEX vector (Amersham Pharmacia Biotech). The purified protein was dialyzed to remove glutathione and treated with thrombin to release GST, and the free GST was removed by adding a second aliquot of glutathione-Sepharose and collecting the unbound fraction as antigen. The murine monoclonal antibody-producing cell lines (HIP1-4B10, HIP1-1B11, and HIP1-1A1) were generated using standard procedures and characterized. The polyclonal antibody to the human HIP1 antigen has been previously described (25).

The rabbit polyclonal mHIP1 antibody was directed against a mHIP1 recombinant protein (mHIP1 amino acids 1 to 533) that was prepared as described for the pGEX-3'HIP1. For the initial immunization, 100 μg of purified antigen was dissoved in complete Freund's adjuvant and injected subcutaneously into a rabbit at multiple sites. Purified antigen (50 μg) was mixed with incomplete Freund's adjuvant and used for the secondary immunizations.

**Cell lines and culture.** Human 293T and A549 cells were grown in Dulbecco's modified Eagle's medium with 10% fetal calf serum.

**Immunofluorescence and confocal microscopy.** Cells grown on coverslips were fixed with 3% formaldehyde in phosphate-buffered saline (PBS) and then permeabilized with 0.1% Triton X-100. After blocking with 1% milk, cells were single or double labeled with various primary antibodies (1:100 in PBS-Tween [PBST]). For HIP1 staining, a mixture of two monoclonal antibodies (4B10 and 1B11) was used. For AP2 staining, cells were incubated with anti α-adaptin rabbit polyclonal antibody (Santa Cruz Biotechnology). Clathrin was identified using anti-clathrin heavy-chain goat polyclonal antibody (Santa Cruz Biotechnology), and eps 15 was identified using anti-eps 15 goat polyclonal antibody (Santa Cruz Biotechnology). The bound antibodies were visualized with anti-mouse immunoglobulin G (IgG) conjugated to fluorescein isothiocyanate (for the monoclonal antibody), anti-rabbit IgG conjugated to Texas Red (for the rabbit polyclonal antibody), or anti-goat IgG Texas Red (for the goat polyclonal antibodies), all at 1:300 in PBST. The fluorescence signals were analyzed under a Zeiss Axioplan epifluorescence microscope or a Zeiss LSM 510 confocal microscope. Images were processed using Adobe Photoshop software.

**Immunoprecipitations.** Protein extracts (500 μg to 1 mg of total protein) from 293T or A549 cells were made by adding lysis buffer A (50 mM Tris [pH 7.4], 150 mM NaCl, 1% Triton X-100, protease inhibitors, 30 mM sodium pyrophosphate, 50 mM NaF, 100 μM sodium orthovanadate) and were incubated at 4°C for 1 h with 5 μl of anti-hHIP1 polyclonal rabbit immune serum (see above). Protein G-sepharose (Pharmacia) was used to precipitate the immune complexes. The protein G beads were washed three times with 500 μl of lysis buffer. Lysis buffer plus 5 mM MgCl$_2$ and 0.5 mM EGTA is described in the legend to Fig. 3.

**Western blotting.** Immunoprecipitates were separated into two aliquots and were separated on two separate sodium dodecyl sulfate–7% polyacylamide gels,
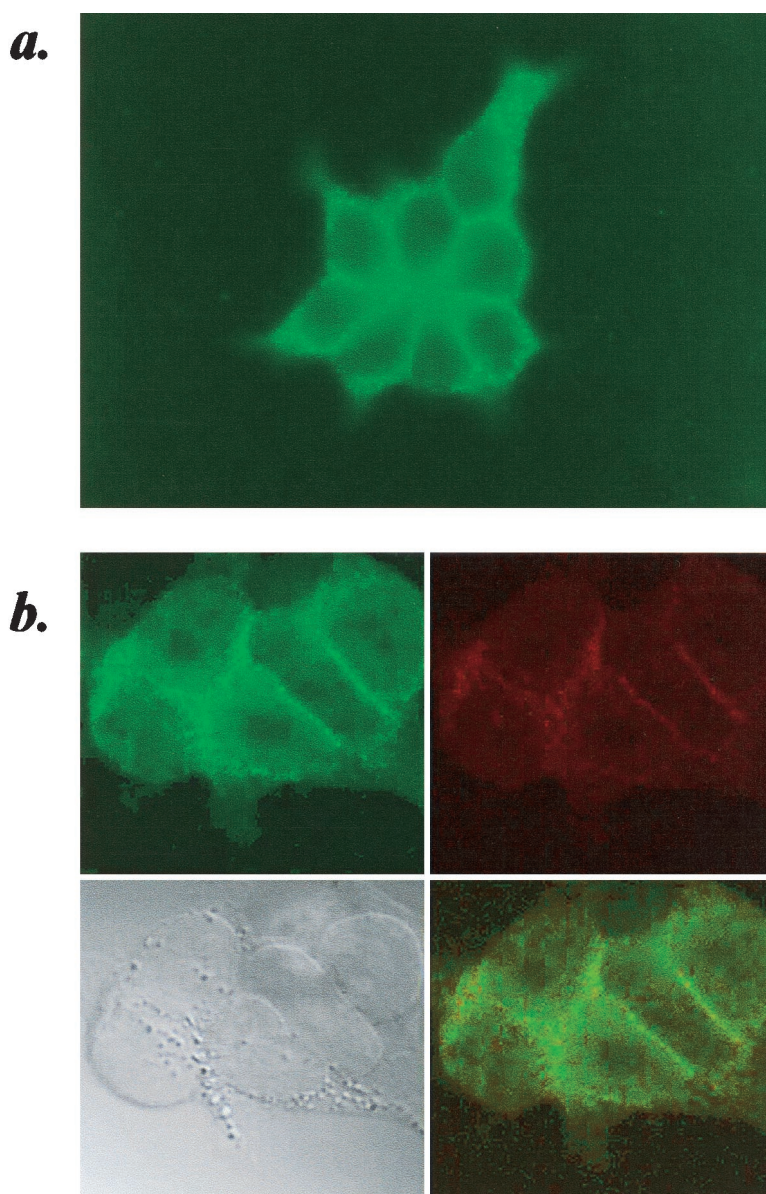
FIG. 2. Immunofluorescence confocal analysis of the intracellular distribution of endogenous hHIP1 (green) in 293T cells and its localization with respect to Eps15 (red). (a) HIP1 is localized to punctate vesicle-like structures. Labeling of HIP1 was done with anti-HIP1 monoclonal antibody 4B10 and anti-mouse FITC secondary antibody. The staining pattern with anti-HIP1 monoclonal antibodies is punctate, and the spots are distributed evenly in the cytoplasm. A similar pattern was obtained using anti-HIP1 polyclonal antibody. All subsequent HIP1 labeling was done with the monoclonal antibodies since there is little background and no signal in the red spectrum. (b) Double labeling of HIP1 (green) and eps15 (red) and overlay of the two (bottom right panel). The differential interference contrast/Nomarski images (bottom left panel) highlight cell morphology and identify the nuclei.

transferred to nitrocellulose (Hybond-ECL, Amersham-Pharmacia), and blocked with TBST–5% bovine serum albumin (BSA). Primary antibodies to clathrin and HIP1 were added to each gel (1:200 for the clathrin monoclonal antibody to 1:5,000 for the HIP1 polyclonal antibody) and were incubated with the blocked membrane in 5% BSA/TBST. The membranes were washed with TBST, and then anti-rabbit horseradish peroxidase-conjugated secondary antibodies (1:5,000 in TBST) were used to develop the blots by ECL.

**Generation of *HIP1*-deficient mice.** The *HIP1* knockout vector (pHIP1KO) was constructed from two mouse genomic clones. Mouse genomic clones were obtained using information from the human genomic structure deduced from the human genomic sequence of the long arm of chromosome 7 (GenBank accession no. AC004491) and the cDNA sequence (Genbank accession no. HS*HIP1*PRO). The mouse genomic clones were isolated from a 129/Sv genomic BAC library for subcloning and restriction mapping. The mouse cDNA used to screen for the genomic clones was obtained by homology screening from a fetal mouse cDNA

library (kindly provided by Lewis Chodosh, University of Pennsylvania). This cDNA was also used to deduce the 5′ end of the *HIP1* cDNA gene and promoter region (see Fig. 1). We subsequently obtained a restriction map of the 5′ end of the gene as one of the HIP1 BAC clones contained exon 2 and the other contained exons 3 to 8. Using these two clones, the targeting vector, pHIP1KO, including the knockout region of approximately 13.7 kb (including exons 2 to 7), was completed. The most 5′ *HIP1* subclone (subclone EcoB/E) was digested with *Xba*I, filled in, and digested with *Xho*I. The resultant 3.5-kb fragment containing intronic sequence 500 bp upstream of the 5′ arm was cloned into the *Nhe*I (blunted)-*Xho*I site of 38LoxPNeo (a modified version of pGT-N38 from New England Biolabs) that has a LoxpNeo cassette cloned into the polylinker. As a result, the 3.5-kb 5′ arm was just 5′ of the LoxPNeo cassette. This intermediate vector was then digested with *Xba*I located 3′ to the Neo cassette and blunted. A subclone (H/B) that contained exon 8 and flanking 5′ and 3′ intronic sequences was digested with *Hin*dIII (the 4.0-kb 3′ arm), which released the entire
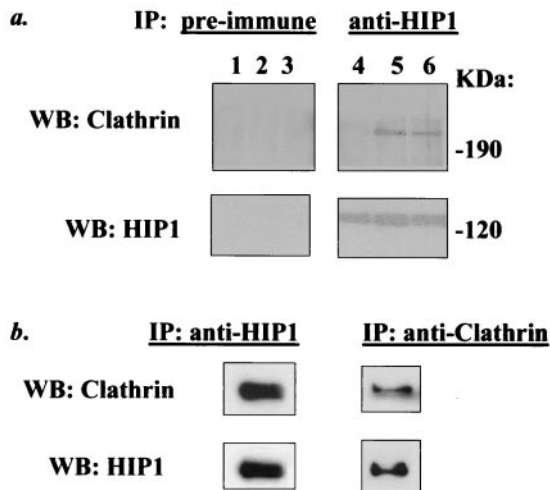
FIG. 3. HIP1 associates with clathrin. (a) Immunologic analysis of 293T cell extracts prepared using various lysis buffers. Lanes: 1, extract prepared with lysis buffer A, immunoprecipitating (IP) antibody pre-immune rabbit serum; 2, extract prepared with lysis buffer B; 3, extract prepared with lysis buffer C; 4, extract prepared with lysis buffer A, immuniprecipitating antibody anti-3′hHIP1 polyclonal antibody; 5, extract prepared with lysis buffer B; 6, extract prepared with lysis buffer C. Lysis buffer A is defined in Materials and methods. Lysis buffer B is the same as buffer A but with 1.5 mM MgCl$_2$, 5 mM EGTA, and 10% glycerol added; lysis buffer C is the same as lysis buffer B without NaCl. (b) Immunologic analysis of A549 lung cancer cell lines for the HIP1 association with clathrin. The immunoprecipitating antibody was the same as in lanes 4 to 6 of panel A. In both panels, the immunoprecipitated proteins were Western blotted (WB) with either anti-clathrin or anti-HIP1 antibodies, as indicated.

4 kb of this subclone. This HindIII fragment was then blunted and ligated with the XbaI (blunted) intermediate vector. The 5′ junction of this resultant vector was sequenced to determine if the 4-kb 3′ arm was in the correct orientation. The final targeting vector was electroporated into 129SvJ RW1 ES cells (Incyte Genomics, St. Louis, Mo.), selected for G418 resistance, and screened by Southern blotting for correctly targeted clones. Generation of chimeric mice and germ line transmission of the mutant allele were achieved using standard techniques.

**Genotypic analysis.** Tail biopsies of 3-week-old mice were performed at weaning. Genomic DNA was isolated using the Promega Wizard kit as specified by the manufacturer digested with EcoRI overnight, and run on a 0.7% agarose–Tris-borate EDTΔ (TBE) gel to separate 16.5-kb (wild type) and 12.0-kb (recombinant) bands detected with the 5′ probe. The gel was then blotted onto Hybond-N filter (Amersham-Pharmacia) and blocked in 20 μg of salmon sperm DNA per ml in hybridization buffer (Amersham-Pharmacia) for 3 h at 65°C. $^{32}$P labeling of the 5′ probe was done by random-primed labeling (Roche) with [$^{32}$P]dCTP (NEN). The blots were then hybridized for 14 to 20 h at 65°C, washed twice in 2× SSC (1× SSC is 0.15 M NaCl plus 0.015 M sodium citrate) for 20 min and twice in 1× SSC for 10 min, and imaged on Kodak Biomax film. Exposures varied from 24 h to 1 week.

**Necropsy and histology.** Mice were sacrificed at 4, 6, 8, 12, 16, 20, and 24 weeks of age. Urogenital tract weights were obtained at necropsy, and testicular tissue was fixed in 10% formalin in PBS (for terminal deoxynucleotidyltransferase-mediated dUTP-bionin nick end labeling [TUNEL] and immunohistochemistry) or Bouin's solution (for routine histology). Tissues were trimmed and embedded in paraffin, and 0.8- μm sections were obtained for routine hematoxylin and eosin staining (described elsewhere), TUNEL, and immunohistochemistry. Histologic scoring was done on hematoxylin-and-eosin-stained sections (see Table 3), and giant cells were counted in duplicate in a fashion that was blind to sample genotype.

**TUNEL and immunohistochemistry.** Slides were deparaffinized twice in xylene for 5 min and rehydrated through a graded ethanol series (100, 95, 90, 80, 70, and 50% for 2 min each), and membranes were permeabilized with 200 μg of proteinase K per ml for 30 min at 37°C. The TUNEL assay was performed using the InSitu cell death detection kit (Roche), using an alkaline phosphatase-conjugated anti-fluorescein dUTP antibody. These were stained with nitroblue

tetrazolium chloride/5-bromo-4-chloro-3-indolylphosphate (NBT-BCIP; Roche) and counterstained with Nuclear Fast Red (Vector Labs). All deep violet cells were counted as TUNEL positive. Immunohistochemistry for germ cell nuclear antigen (GCNA) or human HIP1 was performed by incubating tissue sections with the monoclonal rat IgM 10D9G11 tissue culture supernatant (kindly provided by G. C. Enders, University of Kansas) at full strength or MAb HIP1-4B10 at a 1:1500 dilution for 90 min at 37°C. The primary antibody was then visualized with the ABC Elite kit (Vector Labs) with a peroxidase-conjugated universal secondary antibody and 3,3′-diaminobenzidine (Vector Labs).

**Sperm counts.** Left and right epididymides obtained from freshly necropsied mice were homogenized to a single-cell suspension in PBS. The suspension was then counted on a hemocytometer in duplicate. Sperm counts are expressed as the total number of sperm per epididymis; this represents an average between the left and right epididymis.

**Immunoblot of mouse tissues.** Immediately after removal from mice, brain and testis extracts were prepared by homogenization is in lysis buffer containing protease inhibitors. Extracts (50 μg of total protein) were separated by SDS-polyacrylamide gel electrophoresis 6% polyacrylamide transferred to nitro-cellulose (Hybond-ECL, Amersham-Pharmacia-Biotech), and blocked with TBST–5% BSA. A 1:1,000 dilution of primary anti-mHIP1 polyclonal antibody was incubated with the blocked membrane in 5% nonfat dry milk in TBST. The membranes were washed with TBST, and anti-rabbit horseradish peroxidase-conjugated secondary antibody (1:5000 in TBST) was used to develop the blot by ECL.

## RESULTS

**Genomic organization of *HIP1* and its amino-terminal protein sequence.** During the construction of the targeting vector to knock out HIP1, a human *HIP1* cDNA clone was used to screen a mouse embryonic cDNA library and a 5′ murine *HIP1* clone was isolated. This cDNA clone carried a new exon not previously described. By homology searching, we were able to obtain a high-probability match with a 161-bp region of human chromosome 7q11 (BAC clone CTB-139P11) (Fig. 1a). The first intron separating this newly identified first exon and the second exon spans 139.5 kb. Exon 2 was previously designated exon 1 (14, 28). Unlike exon 2, the newly discovered exon 1 contains a cluster of three in-frame ATG sequences, at +41, +50, and +62 in exon 1 (Fig. 1a), with strong Kozak consensus sequences (15). Initiation of translation from the first ATG sequence found here would result in a HIP1 protein of 116 kDa, consistent with the size observed by Western blot analysis.

Examination of the genomic sequence from BAC clone CTB-139P11 demonstrates a putative promoter region in the 5′-flanking sequence of the open reading frame that begins with *HIP1* exon 1. This region contains a CCAAT box at -71 (Fig. 1a) of exon 1 as well as several GC-rich areas corresponding to GC boxes (Fig. 1a). Furthermore, several putative binding sites for transcription factors were found in this 5′-flanking region, including those for NF-κB, EGR-1, and c-myb.

The predicted protein sequence for exon 1 encodes an additional 42 amino acids, compared with the sequence recorded at the National Center for Biotechnology Information (accession no. XP 004910). Analysis of the predicted protein sequence for full length *HIP1* demonstrates a putative P-4,5-P$_2$ and PI-3,4,5-P$_3$ binding ENTH motif (Fig. 1b), in addition to putative clathrin and AP2 binding sequences (22, 27), a leucine zipper, and a TALIN homology domain (14). The leucine zipper lies within a region that demonstrates homology to the central rod region of intermediate filament proteins (16). These homology domains suggest that HIP1 interacts with both the cytoskeleton and clathrin-coated vesicles.

**HIP1 is associated with clathrin coats.** Together with previous work showing that HIP1r colocalized with clathrin coat
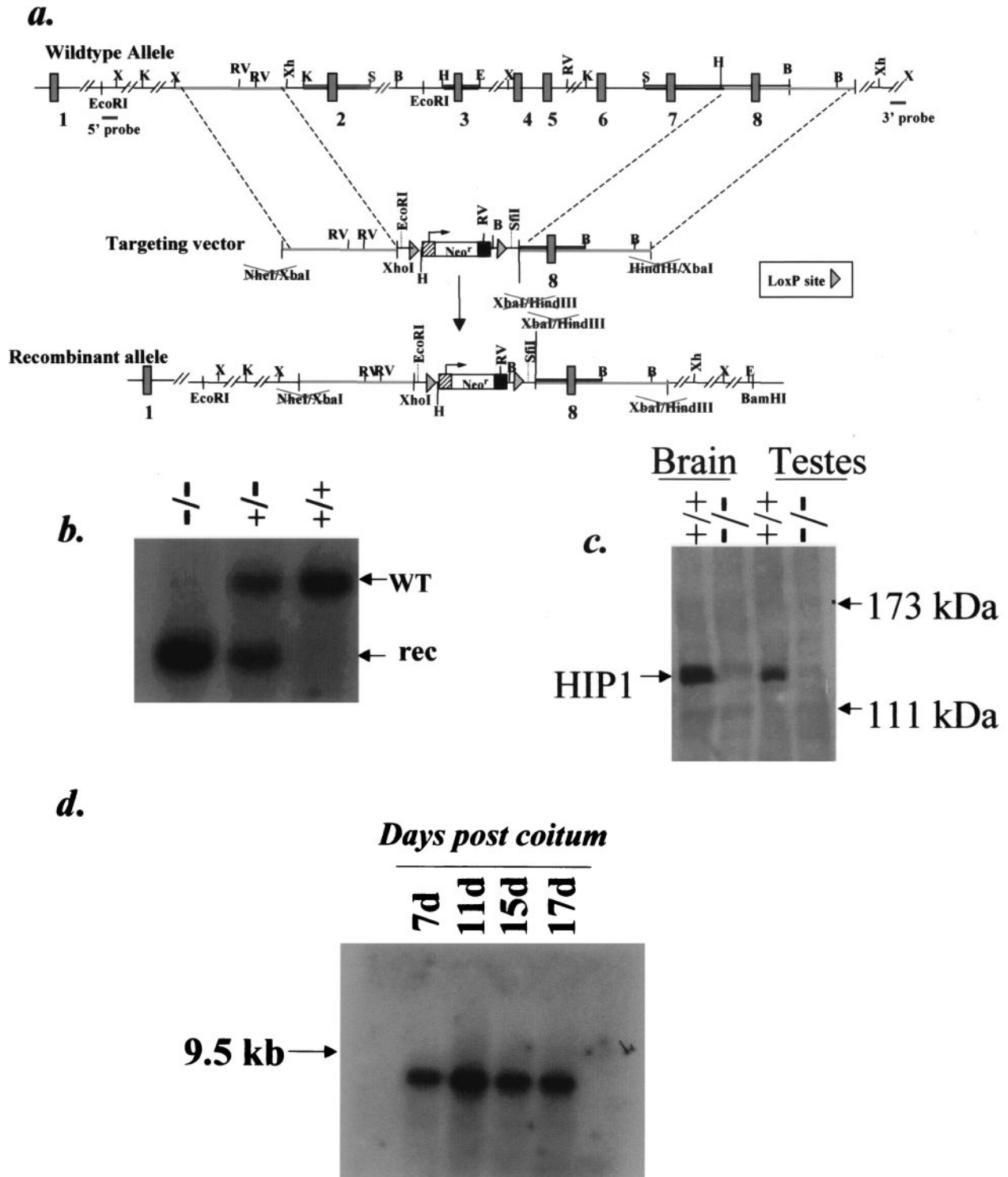
FIG. 4. Targeted disruption of murine *HIP1* by homologous recombination. (a) Targeted deletion of a 13.7-kb segment of the murine *HIP1* gene, including exons 2 to 7. The targeting vector contained a *loxP* flanked Neo<sup>r</sup> cassette. Homologous recombination between the 5′ and 3′ sequences flanking the knockout region results in a recombinant allele with a *loxP*-flanked Neo<sup>r</sup> in the same orientation as *HIP1*. If a transcript were spliced between exons 1 and 8, translation would result in a premature stop codon. Abbreviations: Ap, *Apa*I; B, *Bam*HI; E, *Eco*RI; H, *Hin*dIII; K, *Kpn*I; Sph, *Sph*I; X, *Xba*I. (b) Southern blot analysis of genomic DNA from tail biopsy specimens screened with the 5′ probe. Screening of genomic DNA digested with *Eco*RI with 5′ probe results in 16.5-kb wild-type (WT) and 12.0-kb recombinant (rec) bands. Abbreviations: +/+, wild type; +/−, heterozygote; −/−, homozygote. (c) Western blot analysis of brain and testicular extracts from *HIP1*<sup>+/+</sup> and *HIP1*<sup>−/−</sup> mice. The 111- and 194-kDa marker bands are indicated. The HIP1 band was absent in extracts from *HIP1*<sup>−/−</sup> mice. (d) Northern blot analysis of normal fetal mRNA for wild-type HIP1. The blot was purchased from Clontech and probed with a <sup>32</sup>P-labeled mHIP1 cDNA fragment carrying nucleotides 1 to 1599.

TABLE 1. Genotypic analysis of embryos generated
from $F_1$ intercrosses

| Embryonic postcoital day | No. of embryos | | | |
|---|---|---|---|---|
| | +/+ | +/− | −/− | Total |
| 12.5 | 9 | 15 | 7 | 31 |
| 13.5 | 12 | 35 | 23 | 70 |
| 14.5 | 5 | 10 | 3 | 18 |
| 15.5 | 9 | 28 | 11 | 48 |
| 16.5 | 14 | 27 | 8 | 49 |
| 17.5 | 19 | 53 | 26 | 98 |
| 18.5 | 9 | 38 | 10 | 57 |
| Total | 77 | 206 | 88 | 371 |

proteins (7) and clues from the primary structure of HIP1 (ENTH and actin binding domains), we analyzed the cellular distribution of HIP1 compared to clathrin coat proteins by immunofluorescence confocal microscopy. Labeling of 293T cells with monoclonal antibodies to HIP1 generated a punctate cytoplasmic staining pattern, which was consistently found when any of the three monoclonal antibodies to HIP1 were used (Fig. 2a and data not shown). Double labeling showed partial colocalization of HIP1 with the major clathrin coat components, clathrin and AP-2 (data not shown), and apparently complete colocalization with eps15 (Fig. 2b). eps15 is a major epidermal growth factor receptor kinase substrate and colocalizes with clathrin and AP-2. It is one of the many clathrin-mediated endocytosis cofactors. Other cofactors include epsin, amphiphysin, AP180, and synaptojanin, to name a few (26).

In addition to being colocalized with clathrin coat components, HIP1 physically interacted with clathrin in both 293T cells and the lung cancer cell line A549, by virtue of coimmunoprecipitation of clathrin with HIP1 (Fig. 3). Specificity of the antibody was demonstrated, since the preimmune serum was unable to precipitate either HIP1 or clathrin (Fig. 3a, compare lanes 1 to 3 with lanes 5 and 6). EGTA and Mg were necessary for this interaction (compare, lane 4 with lanes 5 and 6), and freeze-thawing of extracts diminished the interaction (data not shown). Ionic strength was not important to this interaction, since lane 6 shows the same clathrin-HIP1 association in NaCl-free lysis buffer. The interaction of HIP1 with clathrin coat components was also confirmed in the A549 lung cancer cell line (Fig. 3b). Endogeonous AP-2 was also found in the HIP1 immunoprecipitates in both cell lines (data not shown). Since the primary sequence of HIP1 encodes putative clathrin and AP-2 binding sequences, we predict that these interactions

were direct. On the other hand, we did not find an interaction of endogenous HIP1 with eps15 (data not shown). It is likely that the colocalization of HIP1 with eps15 would be indirect, occurring through their common association with AP-2 and clathrin.

**Targeted inactivation of *HIP1* in the mouse.** To further understand the biological role of HIP1 in endocytosis, we deleted the *HIP1* gene in the mouse. The murine *HIP1* gene is composed of 30 exons spanning 220 kb of genomic DNA. To inactivate *HIP1*, exons 2 to 7 were replaced with a neomycin resistance gene (neo$^r$) (Fig. 4a). The targeting vector was used to target 129 Sv embryonic stem (ES) cells. The successful targeting of 1 ES cell clone out of 492 G418-resistant clones was identified by Southern analysis (data not shown). The correctly targeted ES cell clone was injected into C57BL/6 blastocysts. Chimeras with a high percentage of agouti were mated to C57BL/6 females, and $F_1$ agouti pups were genotyped by Southern blotting. We found the expected equal distribution of wild-type and heterozygous mice among the agouti $F_1$ animals (31 +/- to 30 +/+ animals). $F_1$ heterozygotes were subsequently intercrossed to generate $F_2$ animals, which were genotyped at 3 weeks of age (Fig. 4b). The numbers of $HIP1^{-/-}$ mice from this intercross were decreased compared to the expected Mendelian ratios (28% +/+, 50% +/−, and 22% −/− [total of 520 $F_2$ mice]). Western blotting using an antibody that recognizes a peptide encoded by a sequence 3′ of the deleted region of the HIP1 molecule confirmed the lack of expression of HIP1 protein in $HIP1^{-/-}$ brain and testicular extracts (Fig. 4c). Given that HIP1 mRNA is highly expressed in mouse embryos beginning at postcoital day 7 (Fig. 4d), we undertook genetic and pathologic analysis of mouse embryos from postcoital days 12.5 to 18.5. Surprisingly, we found normal Mendelian ratios and normal-appearing embryos (Table 1 and data not shown). In addition, peripheral blood counts were normal (Table 2). No differences were noted in growth rates or adult weights among mice in the $F_2$ generation.

***HIP1*-deficient mice exhibit defects in spermatogenesis.** During comprehensive necropsy and histologic analysis of $F_2$ mice, it was noted that male $HIP1^{-/-}$ mice exhibited testicular degeneration on routine hematoxylin and eosin staining (Fig. 5a to c). Testicular degeneration was associated with the presence of numerous multinucleated giant cells in the seminiferous tubules of the testis. In addition to the multinucleated giant cells, $HIP1^{-/-}$ mice showed decreased numbers of spermatogenic precursors at various stages of development, as well as decreased eosinophilic material in the lumen of the seminiferous tubules (which represents reduced numbers of mature

TABLE 2. Comparison of peripheral blood counts between $HIP1^{+/+}$, $HIP1^{+/−}$, and $HIP1^{-/-}$ mice[a]

| Genotype | No. of mice | Peripheral blood counts[b] | | | | | WBC differentials | | | | |
|---|---|---|---|---|---|---|---|---|---|---|---|
| | | WBC ($10^6$/ml) | RBC ($10^9$/ml) | Hgb (g/dl) | Hct (%) | Plt ($10^6$/ml) | PMNs[c] (%) | Lymphocytes (%) | Eosinophils (%) | Basophils (%) | Monocytes (%) |
| +/+ | 71 | 9.37 ± 0.38 | 9.91 ± 0.14 | 15.8 ± 0.17 | 55.5 ± 0.94 | 813 ± 27 | 20.8 ± 0.81 | 72.7 ± 1.51 | 1.20 ± 0.12 | 0.30 ± 0.04 | 2.93 ± 0.15 |
| +/− | 112 | 9.77 ± 0.31 | 9.90 ± 0.09 | 16.1 ± 0.11 | 56.2 ± 0.60 | 916 ± 34 | 22.8 ± 0.83 | 72.0 ± 1.04 | 1.30 ± 0.14 | 0.32 ± 0.05 | 2.95 ± 0.12 |
| −/− | 51 | 9.38 ± 0.49 | 9.68 ± 0.16 | 16.1 ± 0.17 | 54.9 ± 1.16 | 836 ± 28 | 20.9 ± 1.26 | 73.5 ± 1.56 | 1.46 ± 0.29 | 1.07 ± 0.59 | 3.06 ± 0.21 |

[a] Mean ± standard error of the mean shown. Differences were not statistically significant.
[b] WBC, white blood cells; RBC, red blood cells; Hgb, hemoglobin; Hct, hematocrit; Plt, platelets.
[c] PMN, polymorphonuclear leukocytes.
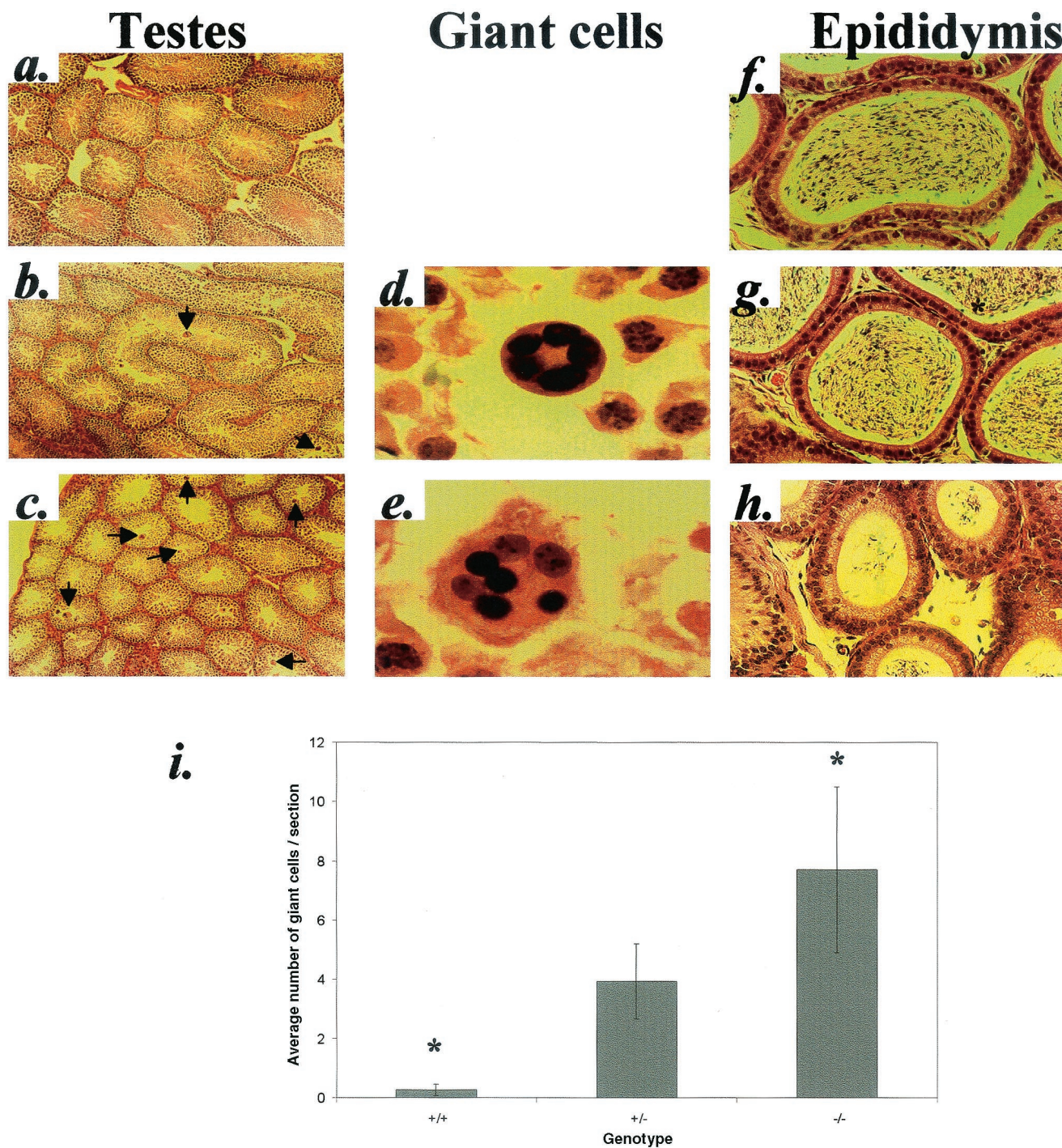
# Testes        # Giant cells        # Epididymis



FIG. 5. Analysis of testes from *HIP1* mutant mice. (a to c) Photomicrographs of testicular sections show seminiferous tubules from 6-week-old +/+, +/−, and −/− animals, stained with hematoxylin and eosin. Arrows in panels b and c show multinucleated giant cells not seen in the testes of +/+ animals. Magnification, ×100. (d and e) High-power photomicrographs of multinucleated giant cells, stained with hematoxylin and eosin. Magnification, ×1,000 under oil immersion. (f to h) Photomicrographs of epidiymides from the same animals in panels a to c. There were fewer mature sperm in the epidiymides of the −/− animal (h). Magnification ×400. (i) Quantitative analysis of the number of giant cells seen on each section (shown as mean and standard error of the mean). Testicular sections ($n$ = 10 to 16 for each genotype) were scored for the number of multinucleated giant cells seen. For +/+ mice, the range was 0 to 2 giant cells/section, while for −/− mice, the number ranged from 2 to 28 giant cells/section. ∗, $P < 0.005$ for comparison between +/+ and −/− mice.

TABLE 3. Histopathological scoring system[a] for evaluation of testicular degeneration

| Criterion | Observation | Score |
|---|---|---|
| No. of giant cells (per section) | 0 to 2 | 0 |
| | 3 to 10 | 1 |
| | 11 to 20 | 2 |
| | 21 to 30 | 3 |
| Eosinophilic material in tubule lumen | >75% of tubules | 0 |
| | 50–75% | 1 |
| | <50% | |
| | Very little or grossly disorganized | 3 |
| Stages of differentiation | All | 0 |
| | Mild reductions in postmeiotic spermatids | 1 |
| | Significant reductions in postmeiotic spermatocytes and spermatids | 2 |
| | Spermatogonia only | 3 |
| Epididymis | Normal | 1 |
| | Oligospermia + debris | 2 |
| | Aspermia | 3 |

[a] The components of the histopathologic scoring system were added and divided by 1.2 if the epididymis was scored and 0.9 if no epididymis was present on the slide. This normalizes the score to a maximum of 10.

sperm) (Fig. 5c). These observations were used as the basis for a histopathologic scoring system to systematically evaluate and quantitate the degree of testicular degeneration (Table 3). $HIP1^{-/-}$ mice showed significantly higher histopathologic scores for testicular degeneration at all ages examined (Table 4). Interestingly, the nuclei present in the giant cells appeared to be derived from spermatids at various stages of maturation (Fig. 5d and e). Many $HIP1^{-/-}$ mice exhibited an absence of mature sperm in the epididymides (Fig. 5f to h). Furthermore, $HIP1^{-/-}$ mice exhibited consistently larger numbers of multinucleated giant cells in the seminiferous tubules ($P < 0.005$ for the comparison between +/+ and −/− mice [Fig.

TABLE 4. Testicular weights, sperm counts, and histopathological scores for +/+, +/−, and −/− mice[a]

| Age (wk) | Genotype | Testicular wt (mg) | Sperm counts ($10^6$) | Histopathologic score (normalized) |
|---|---|---|---|---|
| 6 | +/+ | 79 ± 0.5 | 4.5 ± 0.63 | 1.2 ± 0.30 |
| | +/− | 79 ± 5.3 | 5.6 ± 0.58 | 5.1 ± 0.40 |
| | −/− | 57 ± 2.1* | 0.46 ± 0.18* | 7.9 ± 1.3* |
| 7 | +/+ | 88 ± 3.1 | 7.1 ± 2.9 | 0.42 ± 0.42 |
| | +/− | 90 ± 5.0 | 7.5 ± 0.91 | 1.9 ± 0.83 |
| | −/− | 68 ± 2.2* | 3.9 ± 0.67 | 5.9 ± 0.89* |
| 8 | +/+ | 91 ± 1.3 | 14 ± 2.9 | 0.28 ± 0.28 |
| | +/− | 92 ± 12 | 4.6 ± 1.6 | 1.9 ± 0.84 |
| | −/− | 91 ± 11 | 5.7 ± 1.3 | 3.6 ± 0.32* |
| 20 | +/+ | 97 ± 7.0 | 12 ± 1.2 | 0.67 ± 0.30 |
| | +/− | 98 ± 13 | 13 ± 1.7 | 2.5 ± 0.67 |
| | −/− | 98 ± 8.0 | 11 ± 1.5 | 3.6 ± 0.53* |
| 24 | +/+ | 98 ± 7.8 | 12 ± 0.15 | ND[b] |
| | +/− | 91 ± 8.8 | 12 ± 0.64 | ND |
| | −/− | 92 ± 3.8 | 13 ± 1.9 | ND |

[a] $n$ = 6 to 13 mice were used for each set of comparisons. Results are given as mean ± standard error of the mean. * $P < 0.001$ for comparisons between +/+ and −/− mice.
[b] ND, not done.

TABLE 5. Levels of gonadotropic hormones in serum[a]

| Genotype | Level (ng/ml) of: | | FSH/LH | Level of prolactin (ng/ml) |
|---|---|---|---|---|
| | FSH | LH | | |
| +/+ | 40.5 ± 3.9 | 2.83 ± 0.5 | 16.0 ± 2.8 | 13.5 ± 6.7 |
| +/− | 40.2 ± 8.6 | 2.83 ± 0.7 | 16.1 ± 2.6 | 9.7 ± 3.7 |
| −/− | 43.3 ± 5.8 | 4.29 ± 1.2 | 14.2 ± 3.3 | 14.6 ± 4.1 |

[a] $n$ = 6 for +/+ and −/− animals; $n$ = 7 for +/− animals. Results are given as mean ± standard error of the mean. Differences were not statistically significant.

5f]). It is interesting that $HIP1^{+/-}$ mice had variable evidence of degeneration in the seminiferous tubules, with some animals being completely unaffected and others having a severe phenotype comparable to homozygous-null mice. This phenomenon is seen in other knockout mice that exhibit testicular degeneration and probably results from haploinsufficiency or hemizygosity of the haploid spermatids (5).

To understand the mechanism of testicular degeneration, TUNEL assays were performed to assess the rate of apoptosis in seminiferous tubules (Fig. 6a to c). $HIP1^{-/-}$ mice consistently showed greater numbers of apoptotic cells than did $HIP1^{+/+}$ or $HIP1^{+/-}$ mice in formalin-fixed testicular sections used in these studies ($n$ = 6 for each group; [$P < 0.001$]) (Fig. 6g). These findings provide a partial explanation for the histologic findings. To determine if increased apoptosis affected the stem cell population, an anti-GCNA antibody, which marks spermatogonial stem cells, was used to stain testicular sections (6). No consistent reduction was apparent in the number of spermatogonial progenitors as detected by GCNA staining (Fig. 6d to f).

To evaluate any functional effects of the observed histologic findings, weight measurements of tests and other genitourinary organs from $HIP1^{+/+}$, $HIP1^{+/-}$, and $HIP1^{-/-}$ mice were obtained. The results of these studies are summarized in Table 4. In 6- to 7-week-old $HIP1^{-/-}$ mice, testicular weights were lower than in age-matched $HIP1^{+/+}$ mice ($P < 0.001$). $HIP1^{-/-}$ mice also had lower sperm counts at 6 weeks of age, but the counts were not significantly different in older mice. The normal testicular weights and sperm counts of older $HIP1$-deficient mice contrast with the significantly higher histologic scores observed in all ages of $HIP1$-deficient mice. That is, although testes in HIP1-deficient mice were histologically abnormal at all ages, older $HIP1$-deficient mice were somehow able to compensate for their testicular abnormalities and generate normal numbers of sperm. Perhaps increased proliferation of spermatogonial stem cells eventually compensated for the reduced viability of spermatids in $HIP1$-deficient mice.

To determine whether the phenotype was intrinsic to the testes, we measured follicle-stimulating hormone, luteinizing hormone, and prolactin levels in $HIP1^{-/-}$ mice and their littermates. No significant differences were found between $HIP1^{+/+}$ and $HIP1^{-/-}$ mice (Table 5). In addition, seminal vesicle weights, which are used as surrogate markers for serum testosterone, were not significantly different in $HIP1^{-/-}$ mice from those in $HIP1^{+/+}$ mice. These data suggest that degeneration is intrinsic to the testes and is not mediated by altered hormonal secretion by the pituitary.

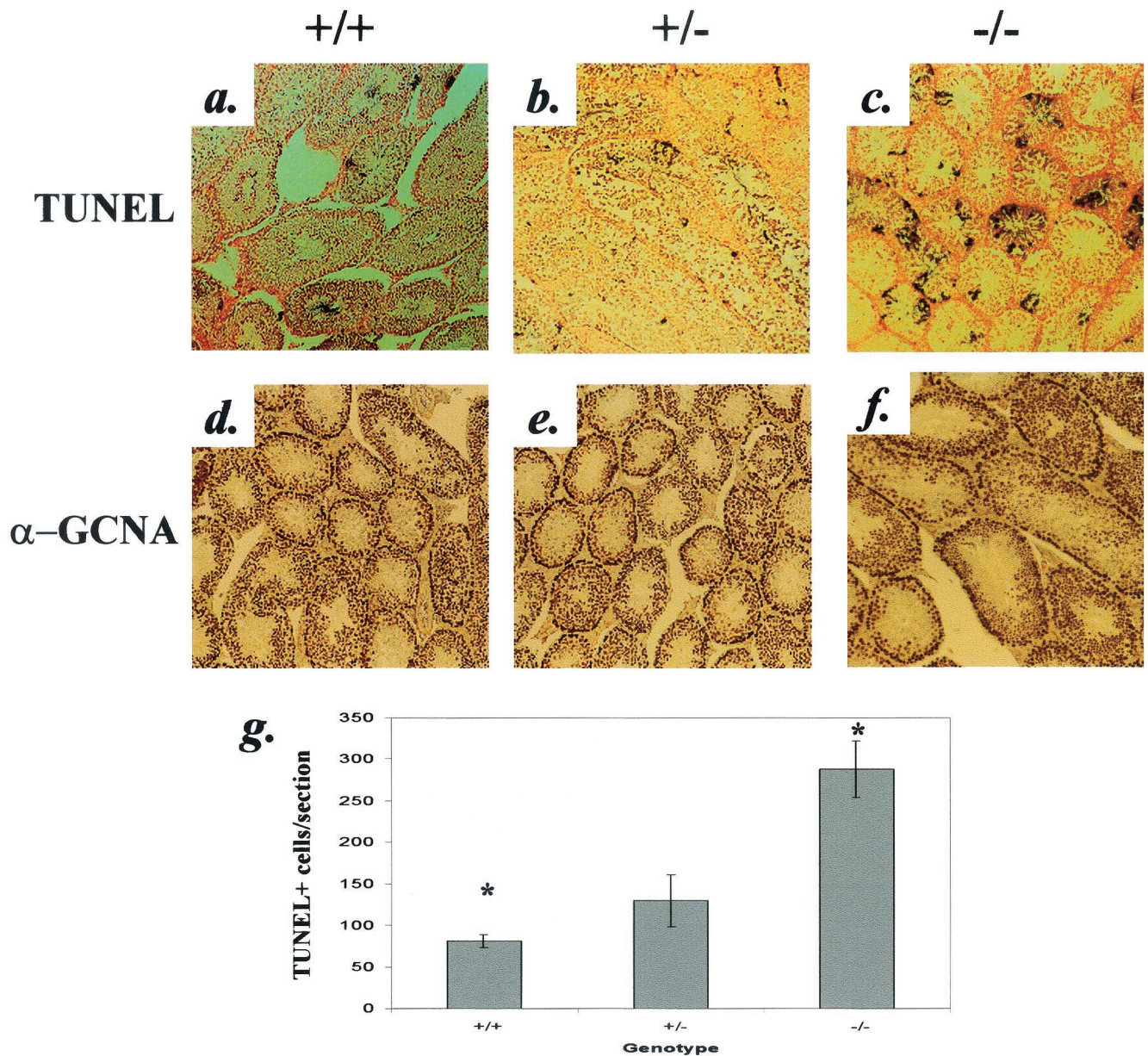In addition to the hormonal data, we have discovered that

FIG. 6. Increased apoptosis in *HIP1*$^{-/-}$ mouse testes without reductions in the spermatogonial cell population. (a to c) Photomicrographs of TUNEL assays in 6-week-old +/+, +/−, and −/− mice, stained with NBT-BCIP and counterstained with Nuclear Fast Red. In the +/+ mice, a few deep violet-black cells were seen (a), but note the large numbers of TUNEL-positive cells seen in the −/− section (c). +/− sections showed a large variability in the number of TUNEL-positive cells (b). All testes were fixed in 10% formalin in PBS for this purpose. Magnification, ×89. (d to f) Immunohistochemical analysis for GCNA. GCNA-positive cells are stained dark brown. No counterstain was used in these sections. There was no difference in the number of GCNA-positive cells among +/+, +/−, and −/− mice. Magnification, ×89. (g) Number of TUNEL-positive cells per section, averaged by genotype (mean and standard error of the mean). Six testicular sections of each genotype were subjected to TUNEL assay, and dark violet-black cells were counted on each section. *, $P<0.001$ for comparison between +/+ and −/− mice.

HIP1 is differentially expressed in seminiferous tubules, arguing for an intrinsic testes defect in the *HIP1*-null mice (Fig. 7). Figure 7a shows a low-power view of human testis stained with anti-HIP1 monoclonal antibody 4B10. Strong staining of the cells in the center of the tubule was noted. Fig. 7b to d are sequentially higher-power views showing that HIP1 is expressed only in the round postmeiotic spermatids. We conclude, therefore, that the lack of HIP1 expression at this par-

ticular stage of spermatogenesis in *HIP1*$^{-/-}$ mice is responsible for the testicular phenotype.

## DISCUSSION

We describe here a novel 5′ first exon and a putative promoter sequence for the *HIP1* gene. This new sequence provided further clues about a role of HIP1 in clathrin-mediated
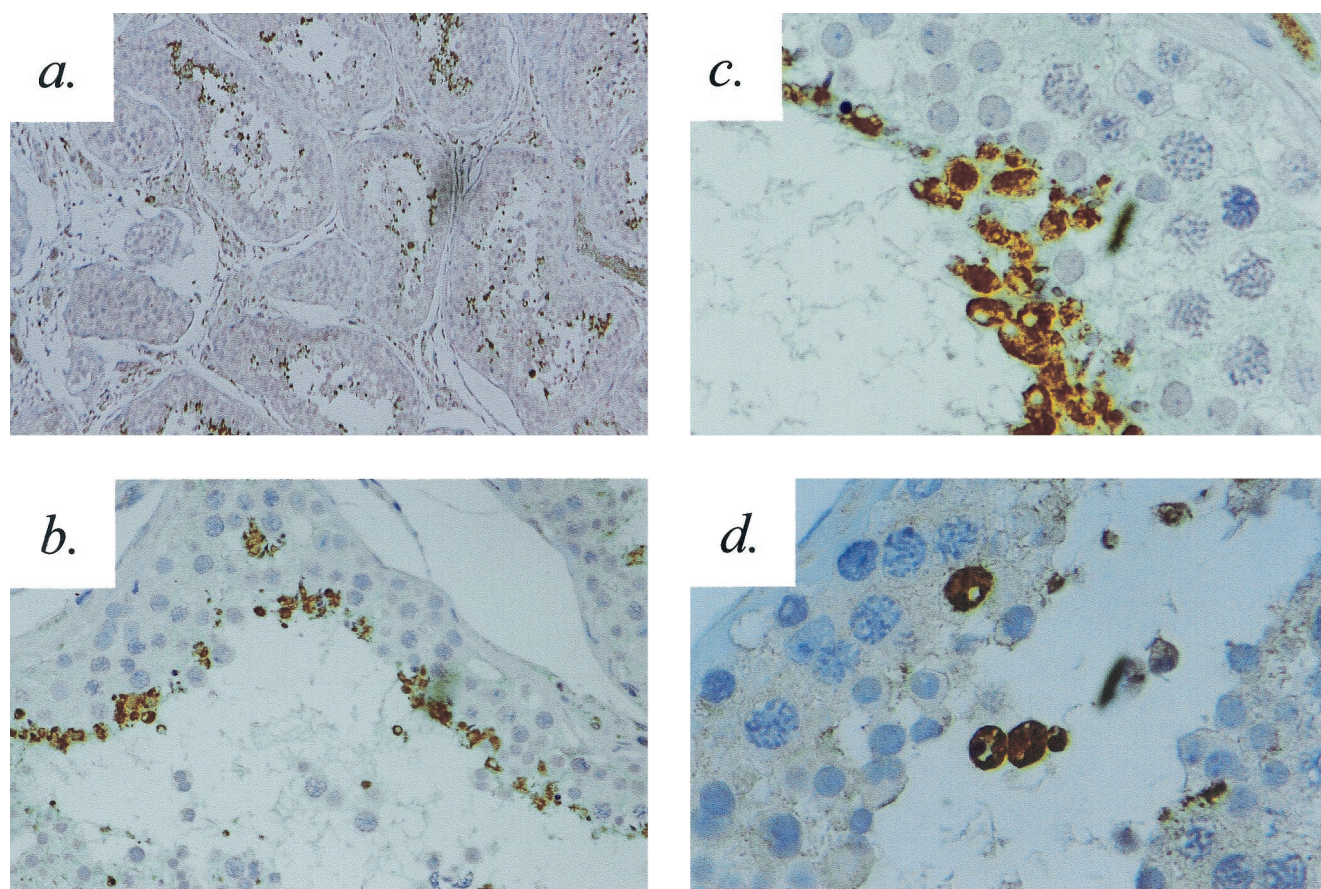
FIG. 7. HIP1 is expressed only in the postmeiotic spermatids of the seminiferous tubules. A monoclonal antibody was generated against a human HIP1 recombinant GST fusion protein and designated HIP1 MAb4B10. Human tissue was fixed in formaldehyde, and standard methods were used to stain with the HIP1 antibody, MAb4B10. (a) Low-power view of the seminiferous tubules showing positive staining (brown) in the center of the tubules. (b to d) Higher-power views ($\times 74$, $\times 296$, and $\times 740$, respectively). demonstrating that only the round postmeiotic spermatids express HIP1. Spermatogonia, primary and secondary spermatocytes, and Sertoli cells do not show expression of HIP1.

endocytosis, since it encodes the initiator methionine that allows the expression of the ENTH domain. In epsin and other related proteins such as HIP1r, this domain interacts with PI-4,5-P$_2$ and PI-3,4,5-P$_3$ and may recruit clathrin and other components of the endocytic machinery to sites of receptor activation (8, 13). In addition to containing ENTH domains, both HIP1 and HIP1r contain TALIN homology domains that typically mediate cytoskeletal interactions by binding actin (7). In this report we provide direct evidence that HIP1 is involved in clathrin-mediated endocytosis by showing that it colocalizes with the clathrin-mediated endocytosis cofactor Eps15 and associates with both clathrin and AP-2 in vivo. This suggests that HIP1 may act as a cofactor in clathrin coat assembly. It is of interest that while other cofactors of clathrin-mediated endocytosis bind AP-2 and clathrin (20, 21), HIP1 also has an actin binding domain and thus may be pivotal in communication between clathrin coated vesicles and the actin cytoskeleton. Thus, HIP1 may link clathrin, the actin cytoskeleton, and the polyphosphoinositide signaling pathway and thereby participate in the regulation of endocytosis.

This is also the first reported knockout of a huntingtin-associated protein. The most remarkable finding in *HIP1*-deficient mice was marked testicular atrophy associated with in-

creased apoptosis of germ cells. The seminiferous tubules of the testes of *HIP1*-null mice showed, in addition to increased programmed cell death, many more giant cells than in wild-type littermates. The testicular phenotype of the *HIP1*-null mice was localized to the postmeiotic spermatids and appeared intrinsic to the testes, consistent with the restricted expression of HIP1 to the postmeiotic spermatids (Fig. 7). Spermatogenic stem cells, Leydig cells, and Sertoli cells of the testes of the HIP1-deficient mice remained intact, and although germ cell development was clearly compromised, the sperm counts of the *HIP1*-null mice were at sufficient levels to maintain fertility.

Spermatogenic stem cells give rise to spermatogonia. Spermatogonia undergo mitosis and differentiate into spermatocytes, which undergo meiosis. These secondary spermatocytes differentiate into spermatids that finally become mature spermatozoa. This maturation sequence requires massive changes in gene expression and cytoskeletal reorganization (4). To our knowledge, this is the first report of a cytoskeletal protein that is required for normal spermatogenesis. However, it is possible that the requirement for HIP1 in spermatogenesis is due to a regulatory rather than a structural role. This is suggested by an analogous phenotype of germ cell apoptosis found in mice with

a targeted deletion of p19$^{Ink4d}$, a cyclin-dependent kinase inhibitor (31).

In addition, a conditional knockout of mouse huntingtin in the testes also causes excess germ cell apoptosis (2). Moreover, mice with knocked-in or transgenic polyglutamine expanded huntingtin with attenuated HIP1 binding (14) exhibit defective spermatogenesis (17; S. Zeitlin, personal communication). This, together with the physical interaction of HIP1 and huntingtin, suggests that HIP1 and huntingtin function in the same biological pathway. Therefore, one possibility is that some of the abnormalities seen with the mutation of *HD* in Huntington's disease may be attributable to the anomalous activity of HIP1 in regulating clathrin-mediated endocytosis. This might have effects on both synaptic vesicle reuptake and growth factor receptor clearance, as discussed below.

HIP1 regulation of endocytosis suggests a mechanism for the abnormalities observed in spermatogenic progenitors. Endocytic clearance of receptor-ligand complexes is an important mechanism that both positively and negatively regulates receptor signaling. On one hand, clearance of activated receptors down-regulates their signaling. On the other hand, recycling of growth factor receptors to the cell surface is necessary to facilitate continued sensitivity of cells to extracellular growth factors. In HIP1-deficient mice, the specificity of spermatogenic progenitors suggests that only particular signaling pathways or particular growth factor receptors depend on HIP1 for adequate function. At the cellular level, it will be important to delineate these pathways. By identifying these HIP1-dependent pathways at the biochemical and cellular levels, it may be possible to uncover important new aspects of how HIP1 affects growth and differentiation.

## ACKNOWLEDGMENTS

## REFERENCES

1. **Dragatsis, I., A. Efstratiadis, and S. Zeitlin.** 1998. Mouse mutant embryos lacking huntingtin are rescued from lethality by wild-type extraembryonic tissues. Development **125:**1529–1539.
2. **Dragatsis, I., M. S. Levine, and S. Zeitlin.** 2000. Inactivation of *Hdh* in the brain and testis results in progressive neurodegeneration and sterility in mice. Nat. Genet. **26:**300–306.
3. **Duyao, M. P., A. B. Auerbach, A. Ryan, F. Persichetti, G. T. Barnes, S. M. McNeil, P. Ge, J. P. Vonsattel, J. F. Gusella, and A. L. Joyner.** 1995. Inactivation of the mouse Huntington's disease gene homolog Hdh. Science **269:**407–410.
4. **Eddy, E. M.** 1998. Regulation of gene expression during spermatogenesis. Semin. Cell Dev. Biol. **9:**451–457.
5. **Eddy, E. M.** 1999. The effects of gene knockouts on spermatogenesis, p. 23–26. *In* C. Gagnon (ed.), The male gamete: applications. Cache River Press, Vienna, Ill.
6. **Enders, G. C., and J. J. May.** 1994. Developmentally regulated expression of a mouse germ cell nuclear antigen examined from embryonic day 11 to adult in male and female mice. Dev. Biol. **163:**331–340.
7. **Engqvist-Goldstein, A. E., M. M. Kessels, V. S. Chopra, M. R. Hayden, and D. G. Drubin.** 1999. An actin-binding protein of the Sla2/Huntingtin interacting protein 1 family is a novel component of clathrin-coated pits and vesicles. J. Cell Biol. **147:**1503–1518.
8. **Ford, M. G., B. M. Pearse, M. K. Higgins, Y. Vallis, D. J. Owen, A. Gibson, C. R. Hopkins, P. R. Evans, and H. T. McMahon.** 2001. Simultaneous binding of PtdIns(4,5)P2 and clathrin by AP180 in the nucleation of clathrin lattices on membranes. Science **291:**1051–1055.
9. **Hackam, A. S., A. S. Yassa, R. Singaraja, M. Metzler, C. A. Gutekunst, L. Gan, S. Warby, C. L. Wellington, J. Vaillancourt, N. Chen, F. G. Gervais, L. Raymond, D. W. Nicholson, and M. R. Hayden.** 2000. Huntingtin interacting protein 1 (HIP-1) induces apoptosis via a novel caspase-dependent death effector domain. J. Biol. Chem. **275:**41299–41308.
10. **Hilditch-Maguire, P., F. Trettel, L. A. Passani, A. Auerbach, F. Persichetti, and M. E. MacDonald.** 2000. Huntingtin: an iron-regulated protein essential for normal nuclear and perinuclear organelles. Hum.Mol.Genet. **9:**2789–2797.
11. **Hirst, J., and M. S. Robinson.** 1998. Clathrin and adaptors. Biochim. Biophys. Acta **1404:**173–193.
12. **Holtzman, D. A., S. Yang, and D. G. Drubin.** 1993. Synthetic-lethal interactions identify two novel genes, SLA1 and SLA2, that control membrane cytoskeleton assembly in *Saccharomyces cerevisiae.* J. Cell Biol. **122:**635–644.
13. **Itoh, T., S. Koshiba, T. Kigawa, A. Kikuchi, S. Yokoyama, and T. Takenawa.** 2001. Role of the ENTH domain in phosphatidylinositol-4,5-bisphosphate binding and endocytosis. Science **291:**1047–1051.
14. **Kalchman, M. A., H. B. Koide, K. McCutcheon, R. K. Graham, K. Nichol, K. Nishiyama, P. Kazemi-Esfarjani, F. C. Lynn, C. Wellington, M. Metzler, Y. P. Goldberg, I. Kanazawa, R. D. Gietz, and M. R. Hayden.** 1997. HIP1, a human homologue of *S. cerevisiae* Sla2p, interacts with membrane-associated huntingtin in the brain. Nat. Genet. **16:**44–53.
15. **Kozak, M.** 1984. Compilation and analysis of sequences upstream from the translational start site in eukaryotic mRNAs. Nucleic Acids Res. **12:**857–872.
16. **Landon, F., M. Lemonnier, R. Benarous, C. Huc, M. Fiszman, F. Gros, and M. M. Portier.** 1989. Multiple mRNAs encode peripherin, a neuronal intermediate filament protein. EMBO J. **8:**1719–1726.
17. **Leavitt, B. R., J. A. Guttman, J. G. Hodgson, G. H. Kimel, R. Singaraja, A. W. Vogl and R. R. Hayden.** 2001. Wild-type huntingtin reduces the cellular toxicity of mutant huntingtin in vivo. Am. J. Hum. Genet. **68:**313–324.
18. **Metzler, M., C. D. Helgason, I. Dragatsis, T. Zhang, L. Gan, N. Pineault, S. O. Zeitlin, R. K. Humphries, and M. R. Hayden.** 2000. Huntingtin is required for normal hematopoiesis. Hum. Mol. Genet. **9:**387–394.
19. **Nasir, J., S. B. Floresco, J. R. O'Kusky, V. M. Diewert, J. M. Richman, J. Zeisler, A. Borowski, J. D. Marth, A. G. Phillips, and M. R. Hayden.** 1995. Targeted disruption of the Huntington's disease gene results in embryonic lethality and behavioral and morphological changes in heterozygotes. Cell **81:**811–823.
20. **Owen, D. J., and J. P. Luzio.** 2000. Structural insights into clathrin-mediated endocytosis. Curr. Opin. Cell Biol. **12:**467–474.
21. **Owen, D. J., Y. Vallis, M. E. Noble, J. B. Hunter, T. R. Dafforn, P. R. Evans, and H. T. McMahon.** 1999. A structural explanation for the binding of multiple ligands by the alpha-adaptin appendage domain. Cell **97:**805–815.
22. **Owen, D. J., P. Wigge, Y. Vallis, J. D. Moore, P. R. Evans, and H. T. McMahon.** 1998. Crystal structure of the amphiphysin-2 SH3 domain and its role in the prevention of dynamin ring formation. EMBO J. **17:**5273–5285.
23. **Ross, T. S., O. A. Bernard, R. Berger, and D. G. Gilliland.** 1998. Fusion of Huntingtin interacting protein 1 to platelet-derived growth factor beta receptor (PDGFbetaR) in chronic myelomonocytic leukemia with t(5;7)(q33;q11.2). Blood **91:**4419–4426.
24. **Ross, T. S., and D. G. Gilliland.** 1999. Transforming properties of the Huntingtin interacting protein 1/platelet-derived growth factor beta receptor fusion protein. J. Biol. Chem. **274:**22328–22336.
25. **Saint-Dic, D., S. C. Chang, G. S. Taylor, M. M. Provot, and T. S. Ross.** 2001. Regulation of the SH2-containing inositol 5-phosphatase SHIP1 in HIP1/PDGFbetaR transformed cells. J. Biol. Chem. **276:**21192–21198.
26. **Slepnev, V. I. and P. De Camilli.** 2000. Accessory factors in clathrin-dependent synaptic vesicle endocytosis. Nat. Rev. Neurosci. **1:**161–172.
27. **Traub, L. M., M. A. Downs, J. L. Westrich, and D. H. Fremont.** 1999. Crystal structure of the alpha appendage of AP-2 reveals a recruitment platform for clathrin-coat assembly. Proc. Natl. Acad. Sci. U.S.A. **96:**8907–8912.
28. **Wanker, E. E., C. Rovira, E. Scherzinger, R. Hasenbank, S. Walter, D. Tait, J. Colicelli, and H. Lehrach.** 1997. HIP-I: a huntingtin interacting protein isolated by the yeast two-hybrid system. Hum. Mol. Genet. **6:**487–495.
29. **White, J. K., W. Auerbach, M. P. Duyao, J. P. Vonsattel, J. F. Gusella, A. L. Joyner, and M. E. MacDonald.** 1997. Huntingtin is required for neurogenesis and is not impaired by the Huntington's disease CAG expansion. Nat. Genet. **17:**404–410.
30. **Zeitlin, S., J. P. Liu, D. L. Chapman, V. E. Papaioannou, and A. Efstratiadis.** 1995. Increased apoptosis and early embryonic lethality in mice nullizygous for the Huntington's disease gene homologue. Nat. Genet. **11:**155–163.
31. **Zindy, F., J. van Deursen, G. Grosveld, C. J. Sherr, and M. F. Roussel.** 2000. INK4d-deficient mice are fertile despite testicular atrophy. Mol. Cell. Biol. **20:**372–378.